International Journal of Engineering Trends and Technology
ISSN: 2231–5381 / https://doi.org/10.14445/22315381/IJETT-V72I3P101
Volume 72 Issue 3, 1-9, March 2024

Original Article

The Use of Random Forest for the Classification of Point Cloud in Urban Scene

Vincenzo Saverio Alfio[1*], Massimiliano Pepe[2], Domenica Costantino[1]

[1]*DICATECh - Department of Civil, Environmental, Land, Building and Chemical Engineering, Polytechnic of Bari, Italy, Bari.*
[2]*InGeo - Department of Engineering and Geology, "G. d'Annunzio" University of Chieti-Pescara, Italy, Pescara.*

[*]*Corresponding Author : vincenzosaverio.alfio@poliba.it*

Received: 28 December 2023 Revised: 18 January 2024 Accepted: 07 February 2024 Published: 17 March 2024

Abstract *- The aim of the paper concerns the classification of the point cloud using a suitable method based on the Random Forest algorithm. In addition, thanks to the use of specific sensors, such as Airborne Laser Scanning (ALS), it is possible to obtain a georeferenced point cloud in a short time, which makes it possible to represent and model urban areas not only through a graphic representation but also through a semantic one. The development of a suitable methodology made it possible to automatically classify a point cloud acquired on an urban scene acquired with a "Leica City Mapper" sensor over the city of Bordeaux (France). The quality of the point cloud classification was evaluated using appropriate performance indices (Overall Accuracy and F1 measure), which showed encouraging results on the quality of the developed method.*

Keywords *- ALS, Random Forest, Point Cloud, Classification, F1 score, Overall Accuracy.*

1. Introduction

The 3D and semantic modelling of urban areas is an interesting and active research topic, as 3D digital models of cities are becoming increasingly common for urban management as a consequence of the growing number of people living in cities [1]. Nowadays, there are an increasing number of techniques and methods for generating 3D models of urban scenes (US) [2-4]. In particular, the use of hybrid aerial sensors consisting of airborne laser scanning (ALS) and nadiral and/or oblique cameras makes it possible to obtain 3D colored point clouds of urban areas in a fast, accurate and detailed manner. Optical and LiDAR systems connected with sensors based on the integration of Global Navigation Satellite System (GNSS) and Inertial Navigation Systems (INS) enable a georeferenced point cloud to be obtained quickly [5]. Starting the point cloud, a very important aspect and one that plays an important role in the management of geospatial data, concerns the classification of the point cloud, i.e. taking the entire data as input and providing it as output, the class to which the initial input belongs. In other words, segmentation aims to classify each point into a specific part of the point cloud [6]. In recent years, several approaches were proposed to classify the point cloud and based on the use of Machine Learning (ML) and Deep Learning (DL). ML and DL fields of application of Artificial Intelligence (AI), based on the development of algorithms that allow computers to make decisions based on initial input data, called training data. Specifically, DL is considered a branch of ML that is based on the use of Artificial Neural Networks (ANNs) with two or more layers (hidden layers) to process information in a non-linear manner [7]. These learning methodologies are generally distinguished into two approaches [8], Supervised Approach and Unsupervised Approaches. In the supervised approach, the Random Forest (RF) algorithm is widely used in the classification of the point cloud. RF is an algorithm that combines the output of several decision tree structures to reach a single result whose ease of use and flexibility have favored its adoption, as it handles both classification and regression problems [9]. RF take as input some manually annotated parts of the point cloud together with so-called "features", attributes of a geometric and/or radiometric nature specially selected by the operator to facilitate the learning and distinction of the classes requested. RF randomly generates several training subsets through the bootstrap sampling method and selects the characteristics of the dataset according to the Gini coefficient to construct a decision tree for each training set to construct a decision tree for each training set; after entering the test sample, the expected result is obtained by calculating the results obtained from all decision trees [10]. The RF algorithm was successfully used in several classification applications. For example, Ni et al., 2020 [11] describe a workflow that, starting from the point cloud derived from airborne laser scanning (ALS), analyses an automation process consisting of the sequential segmentation steps of the point cloud, the subsequent

extraction of geometric features and their RF-based selection and classification, and post-processing. Lu et al. 2022 [12] integrated various data sources and employed a random forest classifier to address spectral similarities between fragmented glacier coverage and surrounding rock and soil, as well as impacts of mountain ranges, cloud cover, and seasonal snowfall shadows during classification tasks.

Aljumaily et al., 2023 [13] introduce the point cloud voxel classification (PCVC) method, an automated, two-step solution for classifying terabytes of data without overwhelming the computational infrastructure; the RF algorithm is then used for the final classification of the object within each voxel using four categories: ground, roof, wall, and vegetation. Therefore, taking into account research developments in the field of point cloud classification, a multiscale method based on the use of ML algorithms applied to cultural heritage is discussed in the paper. In fact, the experiments in the literature mainly concern point clouds acquired from ground platforms and UAVs [14, 15], while the experimentation conducted concerns the acquisition of geospatial data from aerial platforms using hybrid sensors. The algorithms experimented were evaluated on a dataset where the point cloud investigated has a significantly lower density than the datasets present in the literature.

2. ML Classification Algorithms

Many algorithms have been used for ML classification up to the current use of AI and, among the most tested, are Edge-Based, Region Growing, Model Fitting, Hybrid Method and ML applications [16]. In particular, Edge-Based segmentation algorithms involve two main steps, i.e. the localisation of the edge (defined with respect to specific geometric properties) with the aim of delineating the boundaries of two different regions and the grouping of points within the same area, arriving at the final segment. An implementation of this methodology was proposed by Wang et al., 2009 [17], who applied the segmentation algorithm directly on the point cloud with the aim of locating buildings and their separation from vegetation and other layers.

In Region Growing segmentation, the algorithm is based on the analysis of one or more points (seed points) that have common characteristics or features, generating regions that grow around neighboring points with similar characteristics. The Region-Based methods are divided into Bottom-Up approaches, where starting from a few seed points, segments grow on the basis of assigned similarity criteria, and Top-Down approaches, where all the points are assigned to a single region or surface, based mainly on the identification of the seed points and the identification of the features to be associated with the surface, which will subsequently be enlarged to include neighboring points that respect the aforementioned features. In the Model Fitting algorithm approach, artificial objects can be decomposed using simple geometric primitives such as circles, planes, cylinders, etc., by fitting these primitive shapes within the point cloud.

The main model fitting algorithms used are HT (Hough Transform) and RANSAC (RANdom SAmple Consensus) [18, 19]. In Hybrid Methods, several methods are combined in order to exploit the potential of each previous methodology. Tutzauer et al., 2019 [20], for example, propose a feature-based approach for semantic mesh segmentation in an urban scene, using manually computed features and features developed by a 1D convolutional neural network (CNN) typical of DL applications. Through the ML/DL algorithms, typical of AI-related applications, a training process can be initiated in order to develop supervised and unsupervised approaches for the manual or automatic classification of a large amount of input data, respectively. More specifically, algorithms for classifying urban areas and data obtained from ALS sensors classification are rather complex due to the variability and density of the point cloud in different urban areas. In Zeybek, 2020 [15], an approach divided into three main steps and based on the RF algorithm is proposed. Xue et al., 2020 [10] propose the weakly correlated Random Forest by first filtering the cloud through ICSF (Improved Cloth Simulation Filtering) and then introducing the MIC (mutual information coefficient) parameter, constructing an RF with a higher correlation between the various decision trees. Ozdemir et al., 2019 [21] different ML and DL algorithms for the classification of two-point clouds are evaluated, such as OvO ML classifier, BiLSTM, 1D CNN, 2D CNN, and DL classifiers. Under the assumption of point clouds characterized by density variations, presence of noise and high complexity, Yang et al., 2015 [22] and Li et al., 2019 [23] propose a robust and robust approach for the segmentation of point clouds obtained via MLS, combining a novel region growing approach and a multi-size super voxel-based segmentation.

3. Data

The point clouds used in the experimentation are the old city of Bordeaux, in the region of New Aquitaine (France) and in particular in the districts called “Saint Pierre”. The point cloud was obtained from the “Leica CityMapper” hybrid sensor (Leica Geosystems AG—Part of Hexagon AB, Heerbrugg, Switzerland), which is specifically designed for airborne urban mapping. This sensor is equipped with an airborne laser scanner (ALS) and five cameras (one nadir and four oblique) capable of obtaining images of the same target from different angles. In particular, the ALS sensors produce a dense point cloud of the object: the greater the density of the points, the greater the level of detail of the scanned object. Among the parameters that determine the density of the point cloud are the scanning frequency (number of pulses or beams emitted by the laser instrument in 1 second) and the scanning mechanisms (oscillating, sinusoidal, fibre optic, rotating polygon, etc.).

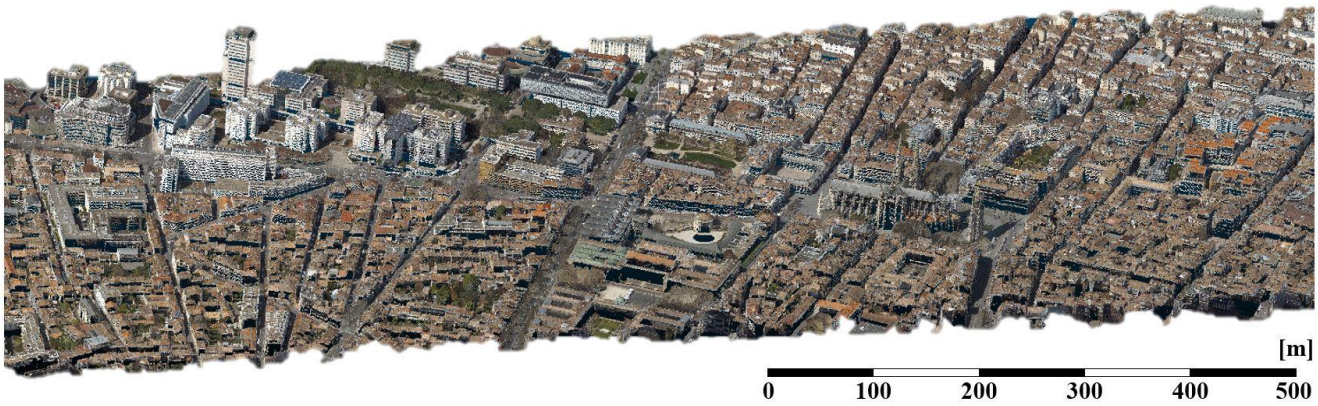

Fig. 1 3D point cloud of the old city of Bordeaux

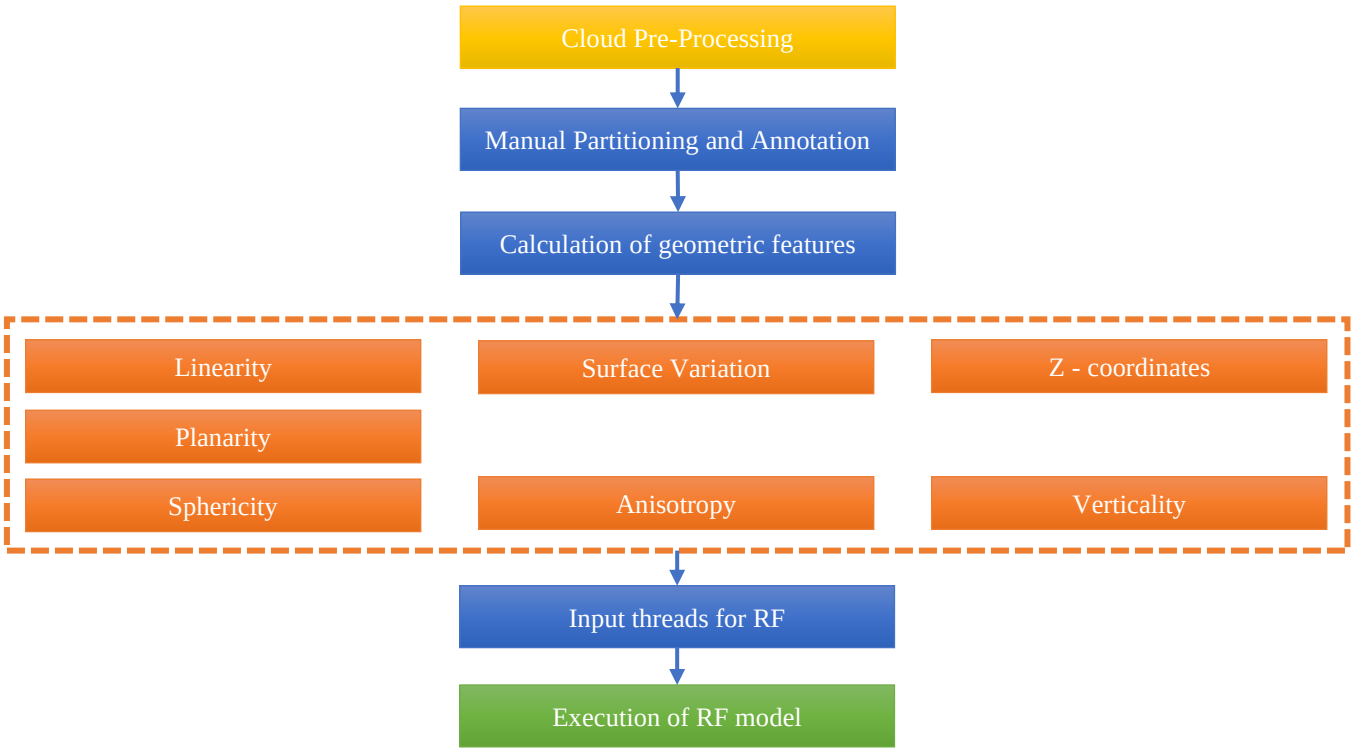

Fig. 2 Pipeline of the developed method.

The definition of the density level of the resulting point cloud determines the pin-pointing activity of the flight mission with ALS sensors. The point cloud consists of approximately 13.5 million points with a density on the horizontal surfaces (roofs and ground) of 7–8 pts/sqm [24]. A 3D view of the colored point cloud Urban Scene is shown in Figure 1.

4. Method

RF automatic classification is a collective learning method for classification, regression and other tasks that operates by constructing a multitude of decision trees at the time of training; the use of this algorithm requires a preliminary processing step related to supervised learning. For a correct identification of the elements of which the urban scene is composed in the point cloud to be classified, it is necessary to define a series of indicators, as the characterization of each point is possible through a combination of geometric and radiometric characteristics. In fact, Linearity, Planarity and Sphericity allow RF to distinguish linear and planar elements (such as the floor or roof) and volumetric elements. Surface variation and anisotropy allow geometric variations in the scene to be identified. In addition, the Z-coordinate and Verticality indexes allow the classifier to distinguish elevation variations and elevation of points. The classification was performed using Cloud Compare (3D point cloud and mesh processing software) and Anaconda (Python programming language distribution platform). In general, the steps necessary for

classification are schematised in the following pipeline (Figure 2). Geometrical characteristics, also known as "covariance characteristics", provide a deeper insight into the geometry of the point cloud, highlighting its discontinuities. These characteristics are expressed by the eigenvalues λ_1, λ_2, λ_3 of the covariance matrix and calculated in a spherical surround of the known radius of the point considered. Through the eigenvalues, it is then possible to determine the geometric features computed in the calculations. According to Mohamed et al., 2021 [25], the geometric features can be calculated from the following relations:

Linearity $$L_\lambda = \frac{\lambda_1 - \lambda_2}{\lambda_1} \quad (1)$$

Planarity $$P_\lambda = \frac{\lambda_2 - \lambda_3}{\lambda_1} \quad (2)$$

Sphericity $$S_\lambda = \frac{\lambda_3}{\lambda_1} \quad (3)$$

Surface Variation $$C_\lambda = \frac{\lambda_3}{\sum \lambda} \quad (4)$$

Anisotropy $$A_\lambda = \frac{\lambda_1 - \lambda_3}{\lambda_1} \quad (5)$$

Verticality $$V = \langle (0,0,1), v_3 \rangle \quad (6)$$

For each test, through a statistical approach, the effectiveness of the classifier was assessed, with respect to overall accuracy, by defining:

- True Positive (TP): number of features that belong to a specific class;
- True Negative (TN): number of features that do not belong to a class but have been wrongly assigned to a class other than their own;
- False Positives (FP): features that do not belong to a class but have been positively predicted for the class;
- False Negatives (FN): features that belong to a class but were not predicted as any class in the image.

In the context of ML, it is possible to define the Confusion Matrix, where each column of the matrix represents the predicted values, while each row represents the actual values. The element on row i and column j represents the number of cases in which the classifier has classified "true" class i as class j, as shown in Figure 3.

Through this matrix, it is possible to represent the statistical classification accuracy using the values of TP/FP and FN/TN. The metrics form a hierarchy that, starting from these definitions of true/false negative/positive, leads to the determination of the parameters up to the evaluation of the following indicators:

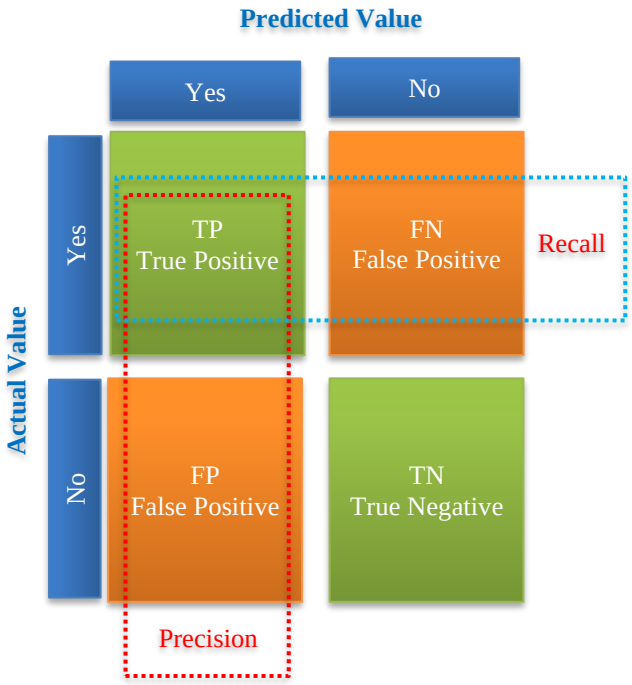

Fig. 3 Representation of the Confusion Matrix

Precision, Overall Accuracy, Recall, and F_1Measure [26-28].

In particular, precision expresses the measure of the number of correct positive predictions (true positives) and can be written as follows:

$$Precision = \frac{TP}{TP + FP} \quad (7)$$

Overall accuracy describes the number of correct forecasts out of all forecasts:

$$OA = \frac{TP + TN}{TP + \mathrm{TN} + FP + FN} \quad (8)$$

Recall measures the number of positive cases the classifier predicted correctly out of all positive cases in the data. It is sometimes also referred to as sensitivity and can be calculated by the equation:

$$Recall = \frac{TP}{TP + FN} \quad (9)$$

Another widely used parameter for point cloud classification is the F_1Measure that combines precision and recall; indeed, it is generally described as the harmonic mean of the two indicators, as it provides a single metric that weights the two ratios (precision and recall) equally, requiring both to have a higher value for the F1-score to increase. The formula of this latter index can be written as follows:

$$F_1\mathrm{Measure} = 2\frac{Precision \cdot Recall}{Precision + Recall} \quad (10)$$

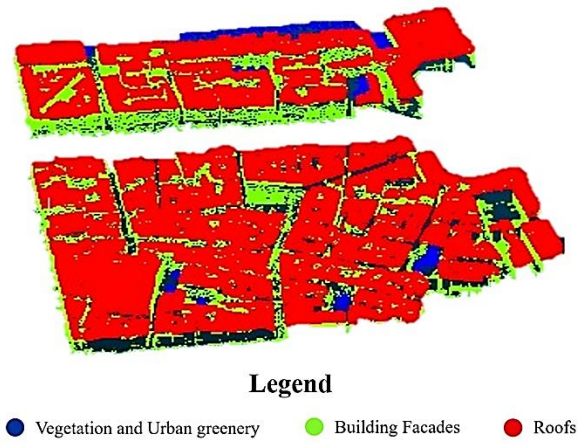

Fig. 4 Type of classes identified in the "Bordeaux" dataset.

5. Experimentation on Datasets

The first fundamental step involves the cleaning of the cloud and, thus, the elimination of noise (outliers). For this operation, we made use of the command in the Cloud Compare plugins known as "Cloth Simulation Filter" [29]. This tool, based on Zhang et al., 2016, makes it possible to automatically remove the soil by initially setting a general parameter on the type of soil (steep terrain, hilly terrain, flat terrain). Then, 3 detailed parameters, in this case left equal to those predefined by the software. The operations of terrain removal and resampling of the cloud were useful to reduce computational time and improve the management of the point cloud. Once this phase has been completed, it is necessary to annotate and thus manually divide the cloud into homogeneous classes. This operation is fundamental because, as input to the classifier, two already annotated portions of the cloud should be provided:

one portion for the supervised learning phase (training) and one portion for evaluating the goodness of the model (evaluation); the latter allows us to evaluate the performance of the model through the confusion matrix and thus the calculation of the precision, recall and F1-score parameters. Manual semantic segmentation was conducted on CC. Initially, both datasets were divided so as to distinguish the part of the cloud intended for classifier training and the part to be classified. The latter portion of the cloud always has a much higher number of points than its counterpart. As mentioned, the part intended for training was further divided and annotated. As for the dataset of the city of Bordeaux, it was first reduced, and only a portion of the initial cloud was subject to classification. The point cloud was then divided, and 3 classes were identified: Vegetation and Urban Greening, Building Facades and Roofs, as shown in Figure 4.

Once the manual annotation phase of the data is completed, it is necessary to evaluate which features to select in order to classify the scene properly. This is the most critical stage of the process because the parameters (resolution and radii of the features) may vary from case to case, depending on the characteristics and dimensions of the objects. However, they correspond to the smallest detail that can be represented at a given scale of representation and its metric tolerance. The approach proposed in the following paper involved the calculation of a total of 40 geometric features. In fact, the 6 chosen features were calculated for different search radii based on the characteristic dimensions of the scenes. In the case of the point cloud on the US of Bordeaux, the spherical contours in which the features were calculated have extremely different search radii. This is related to the characteristic dimensions of the architectural and structural elements that make up the dataset.

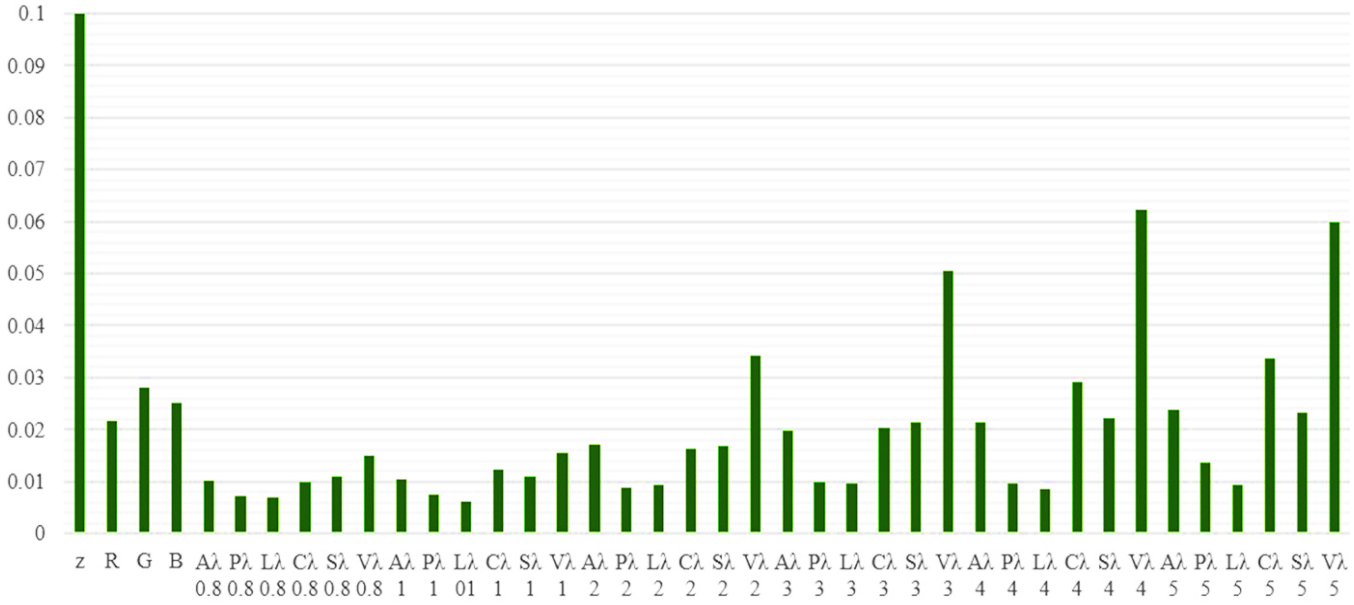

Fig. 5 Ranking of the importance of Test characteristics 1

The following search radii were therefore chosen, as found in Kölle et al., 2021 [30] and Haala et al., 2020 [31]: 0.8 m (for the densest areas of the cloud), 1 m, 2 m, 3 m, 4 m and 5 m. Once the preparation of the datasets is complete, the classifier must be downloaded. In this paper, the RF algorithm proposed by Grilli et al., 2020, available on the web platform (https://github.com/3DOM-FBK/RF4PCC) for developers "GitHub" was used.

The output of the execution of the code was the generation of a .pkl file (related to the number of random trees generated by the classification) and a .txt file containing the dataset for the evaluation with a new column for the predicted classes. In the prompt, it will also be possible to observe a vector called 'feature importance', which allows us to evaluate the most significant features in the training phase and the "confusion matrix"

6. Results

Four tests were conducted on this point cloud. Forty features were provided to the classifier as input, and then a number of 28, 15 and finally 8 features were selected each time. The results obtained after Test 1 are represented in the following Figure 5.

Features that have been removed have a value of less than 0.01. The classification produced the following confusion matrix (Table 1). In addition, three other tests were performed, as described above; in particular, test 4 produced the following confusion matrix (Table 2).

The classified point cloud is displayed in Cloud Compare software (Figure 6): As done for the other datasets, the OA parameter was calculated for each test (Figure 7). In addition, based on the average F1-SCORE values obtained from the various confusion matrices, it was possible to diagram both the trend of the F1 parameter and the trend of the computational times according to the number of features input to the classifier (Figure 8).

Table 1. Confusion matrix for test 1

ID Class	0	1	2	Precision [%]	Recall [%]	F1-score [%]
0	2524	1155	190	65.24	19.50	30.02
1	8373	37118	5590	72.66	44.36	55.08
2	2047	45402	376244	88.80	98.49	93.39
AVERAGE				**75.57**	**54.12**	**59.50**
TRAINING TIME: **655.17 s** CLASSIFICATION TIME: **71.11s** N. FEATURES: **40** ACCURACY: **86.89%**						

Table 2. Confusion matrix for test 4

ID Class	0	1	2	Precision [%]	Recall [%]	F1-score [%]
0	3035	1343	364	64.00	15.42	24.85
1	13198	81945	6871	80.33	56.24	66.16
2	3450	62427	382550	85.31	98.14	91.28
AVERAGE				**76.55**	**56.60**	**60.76**
TRAINING TIME: **249.86 s** CLASSIFICATION TIME: **33.42s** N. FEATURES: **8** ACCURACY: **84.21%**						

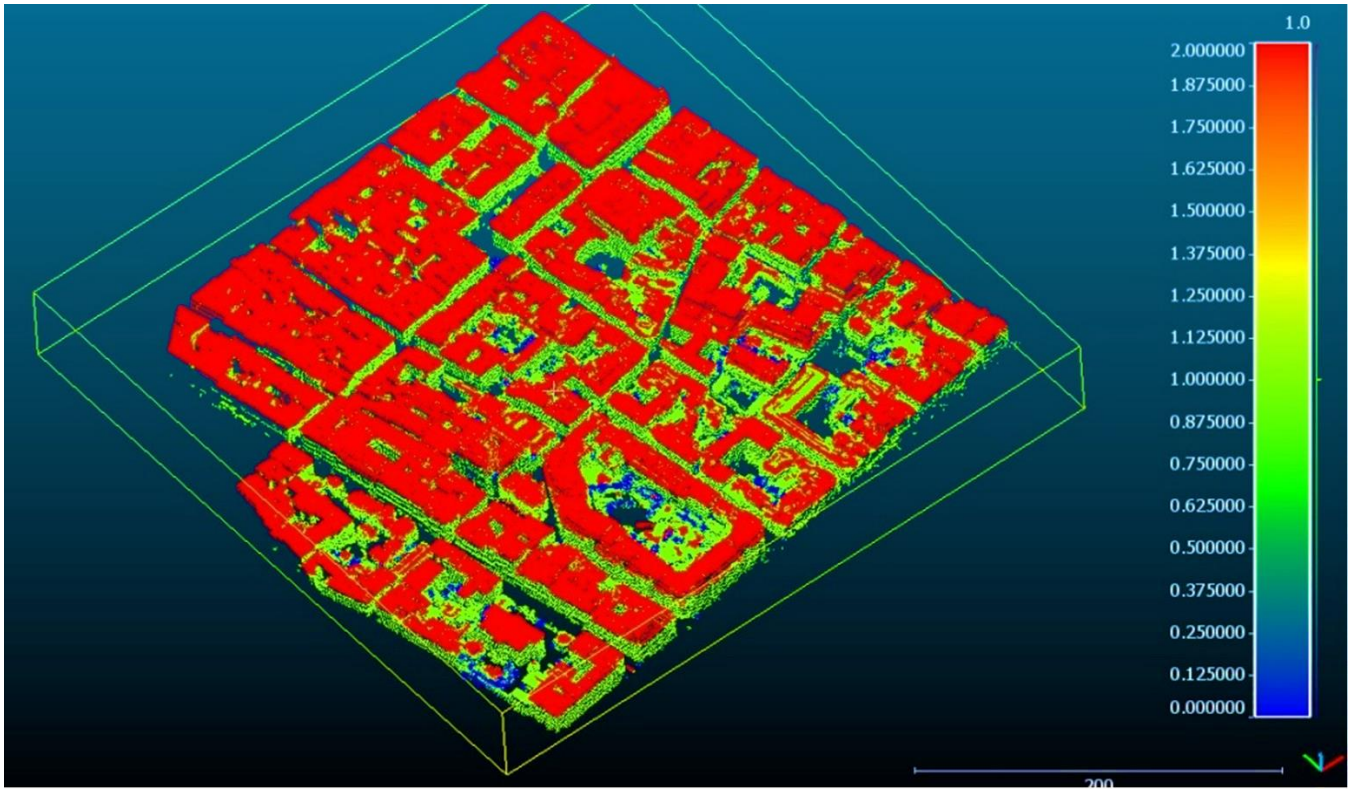

Fig. 6 Classified point cloud of the historic city centre of Bordeaux

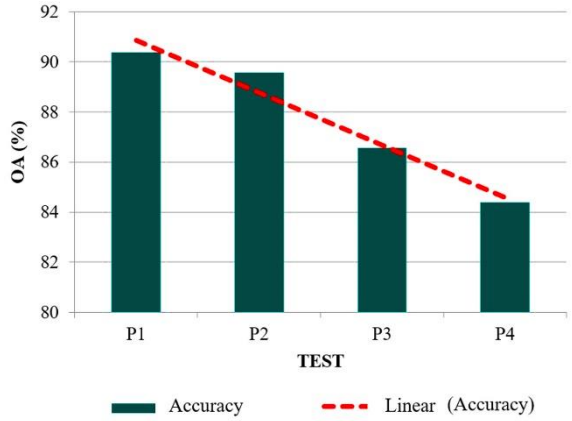

Fig. 7 OA values in the several tests

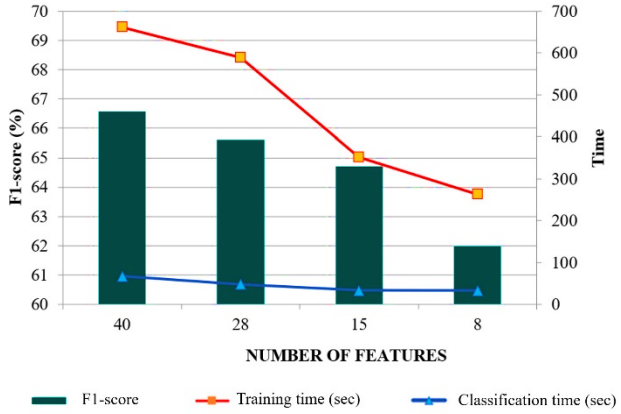

Fig. 8 Classification results with different features

7. Discussions

The results obtained on the dataset of the metropolitan city of Bordeaux demonstrate how the proposed approach allows a semantic classification of the point cloud. It is possible to observe, from Figures 7 and 8, how the first test performed achieved a value relative to the OA parameter of 90.3% and an F1-score of 66.5%, respectively. It can also be seen, observing from the linear interpolation line on both the OA and F1-score, that as the number of features input to the classifier decreases, the parameter decreases linearly.

The reasons for these negative trends are to be attributed mainly to the recall and precision parameters; in fact, observing the confusion matrices of the various tests carried out, it can be seen that as the number of features decreases, the classifier increasingly confuses first class 0 (vegetation) and class 1 (façades) and then class 1 and class 2 (roofs). This shows how in transition zones between very dense areas, where there are public green, and less dense areas, such as facades, RF classifies many points incorrectly.

The same applies in the transition zones between building façades (not very dense point cloud) and building roofs (very dense point cloud). Furthermore, taking the feature vector "importance" of tests 1 and 2 into consideration, it is easy to see how the features chosen to allow the classifier not to misclassify points in areas of varying density become unimportant.

For this reason, geometric features were also calculated in a spherical surround of a radius of 0.8 m in order to allow the classifier to distinguish high-density zones from low density zones. Finally, a further important aspect to take into consideration concerns the computational time, i.e. as the number of features increases, the classification time also increases. In particular, as shown in test 4, as the "training time" (decrease in the number of features) decreases, the accuracy decreases in an important and decisive way for a suitable classification of the urban scene.

8. Conclusion

The proposed method based on the use of the Random Forest algorithm and a multiscale, reiterative approach resulted in a good classification of the point cloud acquired by the hybrid sensor. Indeed, the performance indices (OA and F1-score) used to assess the quality of the classification showed encouraging results. The OA achieved was about 85%, which is comparable with the existing literature. In addition, it was also possible to see how the density of the resampled cloud positively influences the calculation time and affects the overall accuracy and F1-score by a few fractions of a percent. The results obtained on the Urban Scene of Bordeaux show that the classification carried out with the approach proposed and evaluated in this paper is only valid with the 40 features as input to the classifier. It is, therefore, clear that for extremely complex datasets, such as the urban ones, it is necessary to identify features suitable for the multiscale reiterative search and selection methodology.

References

[1] Valeria-Ersilia Oniga et al., "3D Modeling of Urban Area Based on Oblique UAS Images-An End-to-End Pipeline," *Remote Sensing*, vol. 14, no. 2, pp. 1-31, 2022. [CrossRef] [Google Scholar] [Publisher Link]

[2] Surendra Pal Singh, Kamal Jain, and V. Ravibabu Mandla, "3D Scene Reconstruction from Video Camera for Virtual 3D City Modeling," *American Journal of Engineering Research*, vol. 3, no. 1, pp. 140-148, 2014. [Google Scholar] [Publisher Link]

[3] Lipeng Gao et al., "Novel Framework for 3D Road Extraction Based on Airborne LiDAR and High-Resolution Remote Sensing Imagery," *Remote Sensing*, vol. 13, no. 23, pp. 1-22, 2021. [CrossRef] [Google Scholar] [Publisher Link]

[4] Massimiliano Pepe, Vincenzo Saverio Alfio, and Domenica Costantino, "UAV Platforms and the SfM-MVS Approach in the 3D Surveys and Modelling: A Review in the Cultural Heritage Field," *Applied Sciences*, vol. 12, no. 24, pp. 1-35, 2022. [CrossRef] [Google Scholar] [Publisher Link]

[5] Massimiliano Pepe, Luigi Fregonese, and Nicola Crocetto, "Use of SfM-MVS Approach to Nadir and Oblique Images Generated throught Aerial Cameras to Build 2.5 D Map and 3D Models in Urban Areas," *Geocarto International*, vol. 37, no. 1, pp. 120-141, 2022. [CrossRef] [Google Scholar] [Publisher Link]

[6] Kuangen Zhang et al., "Linked Dynamic Graph CNN: Learning on Point Cloud via Linking Hierarchical Features," *arXiv*, 2019. [CrossRef] [Google Scholar] [Publisher Link]

[7] Eleonora Grilli, "Automatic Texture- and Geometry-based Classification Methods Applied to Cultural Heritage," *Bulletin of the Italian Society of Photogrammetry and Topography*, no. 1, pp. 8-16, 2019. [Google Scholar] [Publisher Link]

[8] Eleonora Grilli, and Fabio Remondino, "Machine Learning Generalisation across Different 3D Architectural Heritage," *ISPRS International Journal of Geo-Information*, vol. 9, no. 6, pp. 1-19, 2020. [CrossRef] [Google Scholar] [Publisher Link]

[9] Leo Breiman, "Random Forests," *Machine Learning*, vol. 45, pp. 5-32, 2001. [CrossRef] [Google Scholar] [Publisher Link]

[10] Doudou Xue et al., "An Improved Random Forest Model Applied to Point Cloud Classification," *IOP Conference Series: Materials Science and Engineering*, vol. 768, no. 7, pp. 1-6, 2019. [CrossRef] [Google Scholar] [Publisher Link]

[11] Huan Ni, Xiangguo Lin, and Jixian Zhang, "Classification of ALS Point Cloud with Improved Point Cloud Segmentation and Random Forests," *Remote Sensing*, vol. 9, no. 3, pp. 1-34, 2017. [CrossRef] [Google Scholar] [Publisher Link]

[12] Yijie Lu et al., "Integration of Optical, SAR and DEM Data for Automated Detection of Debris-Covered Glaciers over the Western Nyainqentanglha Using a Random Forest Classifier," *Cold Regions Science and Technology*, vol. 193, 2022. [CrossRef] [Google Scholar] [Publisher Link]

[13] Harith Aljumaily et al., "Point Cloud Voxel Classification of Aerial Urban LiDAR using Voxel Attributes and Random Forest Approach," *International Journal of Applied Earth Observation and Geoinformation*, vol. 118, pp. 1-13, 2023. [CrossRef] [Google Scholar] [Publisher Link]

[14] Meida Chen et al., "3D Photogrammetry Point Cloud Segmentation using a Model Ensembling Framework," *Journal of Computing in Civil Engineering*, vol. 34, no. 6, 2020. [CrossRef] [Google Scholar] [Publisher Link]

[15] Mustafa Zeybek, "Classification of UAV Point Clouds by Random Forest Machine Learning Algorithm," *Turkish Journal of Engineering*, vol. 5, no. 2, pp. 48-57, 2021. [CrossRef] [Google Scholar] [Publisher Link]

[16] E. Grilli, F. Menna, and F. Remondino, "A Review of Point Clouds Segmentation and Classification Algorithms," *The International Archives of the Photogrammetry, Remote Sensing and Spatial Information Sciences*, vol. 42, pp. 339-344, 2017. [CrossRef] [Google Scholar] [Publisher Link]

[17] Jun Wang, and Jie Shan, "Segmentation of LiDAR Point Clouds for Building Extraction," *American Society for Photogrammetry Remote Sensing Annual Conference, Baltimore*, MD, pp. 1-13, 2009. [Google Scholar]

[18] Lina Yang et al., "Efficient Plane Extraction using Normal Estimation and RANSAC from 3D Point Cloud," *Computer Standards & Interfaces*, vol. 82, 2022. [CrossRef] [Google Scholar] [Publisher Link]

[19] Wei Song et al., "CNN-Based 3D Object Classification using Hough Space of LiDAR Point Clouds," *Human-Centric Computing and Information Sciences*, vol. 10, 2020. [CrossRef] [Google Scholar] [Publisher Link]

[20] P. Tutzauer, D. Laupheimer, and N. Haala, "Semantic Urban Mesh Enhancement Utilizing a Hybrid Model," *ISPRS Annals of the Photogrammetry, Remote Sensing and Spatial Information Sciences*, vol. 4, pp. 175-182, 2019. [CrossRef] [Google Scholar] [Publisher Link]

[21] E. Özdemir, F. Remondino, and A. Golkar, "Aerial Point Cloud Classification with Deep Learning and Machine Learning Algorithms," *The International Archives of the Photogrammetry, Remote Sensing and Spatial Information Sciences*, vol. 42, pp. 843-849, 2019. [CrossRef] [Google Scholar] [Publisher Link]

[22] Bisheng Yang et al., "Hierarchical Extraction of Urban Objects from Mobile Laser Scanning Data," *ISPRS Journal of Photogrammetry and Remote Sensing*, vol. 99, pp. 45-57, 2015. [CrossRef] [Google Scholar] [Publisher Link]

[23] Yuan Li, Bo Wu, and Xuming Ge, "Structural Segmentation and Classification of Mobile Laser Scanning Point Clouds with Large Variations in Point Density," *ISPRS Journal of Photogrammetry and Remote Sensing*, vol. 153, pp. 151-165, 2019. [CrossRef] [Google Scholar] [Publisher Link]

[24] Domenica Costantino et al., "Strategies for 3D Modelling of Buildings from Airborne Laser Scanner and Photogrammetric Data Based on Free-Form and Model-Driven Methods: The Case Study of the Old Town Centre of Bordeaux (France)," *Applied Sciences*, vol. 11, no. 22, pp. 1-24, 2021. [CrossRef] [Google Scholar] [Publisher Link]

[25] M. Mohamed, S. Morsy, and A. El-Shazly, "Machine Learning for Mobile LIDAR Data Classification of 3D Road Environment," *The International Archives of the Photogrammetry, Remote Sensing and Spatial Information Sciences*, vol. 44, pp. 113-117, 2021. [CrossRef] [Google Scholar] [Publisher Link]

[26] Massimiliano Pepe, and Cluadio Parente, "Burned Area Recognition by Change Detection Analysis using Images Derived from Sentinel-2 Satellite: The Case Study of Sorrento Peninsula, Italy," *Journal of Applied Engineering Science*, vol. 16, no. 2, pp. 225-232, 2018. [CrossRef] [Google Scholar] [Publisher Link]

[27] Shamsudeen Temitope Yekeen, Abdul-Lateef Balogun, and Khamaruzaman B. Wan Yusof, "A Novel Deep Learning Instance Segmentation Model for Automated Marine Oil Spill Detection," *ISPRS Journal of Photogrammetry and Remote Sensing*, vol. 167, pp. 190-200, 2020. [CrossRef] [Google Scholar] [Publisher Link]

[28] Massimiliano Pepe et al., "A Novel Method Based on Deep Learning, GIS and Geomatics Software for Building a 3D City Model from VHR Satellite Stereo Imagery," *ISPRS International Journal of Geo-Information*, vol. 10, no. 10, pp. 1-17, 2021. [CrossRef] [Google Scholar] [Publisher Link]

[29] Daniel Girardeau-Montaut, "*CloudCompare*," France: EDF R&D Telecom ParisTech, 2016. [Google Scholar]

[30] Michael Kölle et al., "The Hessigheim 3D (H3D) Benchmark on Semantic Segmentation of High-Resolution 3D Point Clouds and Textured Meshes from UAV LiDAR and Multi-View-Stereo," *ISPRS Open Journal of Photogrammetry and Remote Sensing*, vol. 1, pp. 1-11, 2021. [CrossRef] [Google Scholar] [Publisher Link]

[31] N. Haala et al., "Hybrid Georeferencing, Enhancement and Classification of Ultra-Highresolution UAV LiDAR and Image Point Clouds for Monitoring Applications," *ISPRS Annals of the Photogrammetry, Remote Sensing and Spatial Information Sciences*, vol. 2, pp. 727-734, 2020. [CrossRef] [Google Scholar] [Publisher Link]